

BEAM COMMISSIONING OF SuperKEKB RINGS AT PHASE 1

M. Tobiya^{*}, M. Arinaga, J. W. Flanagan, H. Fukuma, H. Ikeda, H. Ishii, K. Mori, E. Mulyani¹,
 M. Tejima, KEK Accelerator Laboratory, 1-1 Oho, Tsukuba 305-0801, Japan
¹also at SOKENDAI (The Graduate University for Advanced Studies), 1-1 Oho, Tsukuba, Japan
 G.S. Varner, U. Hawaii, Dept. Physics and Astronomy, 2505 Correa Rd., Honolulu HI 96822 USA
 G. Bonvicini, Wayne State U., 135 Physics Bldg., Detroit MI 48201, USA

Abstract

The Phase 1 commissioning of SuperKEKB rings without superconducting final focus magnets or Belle-II detector began in Feb., 2016. A total of 1010 mA (LER) and 870 mA (HER) stored beam has been achieved close to the design emittance and x-y coupling. Most of the beam diagnostics, including new systems such as gated turn-by-turn monitors and X-ray beam size monitors, have been commissioned with beam and proved to be essential to the success of machine commissioning. The results of the beam commissioning, including the evaluation and difficulties of the beam diagnostics are shown.

INTRODUCTION

The KEKB collider has been upgraded to the SuperKEKB collider with a final target of 40 times higher luminosity than that of KEKB. It consists of a 7 GeV high energy ring (HER, electrons) and a 4 GeV low energy ring (LER, positrons). About 2500 bunches per ring will be stored at total beam currents of 2.6 A (HER) and 3.6 A (LER) in the final design goal.

The first stage of commissioning (Phase 1 operation) without the Belle-II detector started in Feb. 2016 and continued until the end of June [1]. The major purposes of this operation were start-up of each hardware components, establishment of beam operation software and tools, low-emittance and x-y coupling tuning, and background studies with the BEAST detector. The Belle-II group requested an integrated beam dose of 360 to 720 Ah to achieve a very low beam-gas background when the Belle-II detector is installed at Phase 2.

The beam instrumentation has played a very important role at each step of commissioning, such as establishing the circulating orbit in the very early stage of commissioning, accumulating large beam currents, and so on. At the same time the performance of the beam instrumentations has been evaluated by the beam.

In this paper we describe the results of the beam commissioning of SuperKEKB rings with the obtained performance of the beam instrumentations. The main parameters of the Phase 1 operation of SuperKEKB HER/LER and the types and number of main beam instrumentations are shown in Table 1.

OUTLINE OF THE COMMISSIONING

Figure 1 shows the Phase 1 commissioning history [2].

^{*} email address: makoto.tobiya@kek.jp

Table1: Main Parameters and Beam Instrumentations of SuperKEKB HER/LER in Phase 1 Operation

	HER	LER
Energy (GeV)	7	4
Circumference(m)	3016	
Max. Beam current (mA)	1010	870
Max. Number of bunches	2455	2363
Single bunch current (mA)	1.04	1.44
Min. bunch separation(ns)	4	
Bunch length (mm)	5	6
RF frequency (MHz)	508.887	
Harmonic number (h)	5120	
Betatron tune (H/V)	44.54/46.56	45.54/43.56
Synchrotron tune	0.02	0.018
T. rad. damping time (ms)	58	43
L. rad. damping time (ms)	29	22
x-y coupling (%)	0.27	0.28
Natural emittance (nm)	3.2	4.6
Beam position monitor	486	444
BPM Displacement sensor	110	108
Gated turn-by-turn monitor	58	59
Transverse FB system	2	2
Longitudinal FB system	0	1
Visible SR size monitor	1	1
X-ray size monitor	1	1
Betatron tune monitor	2	2
DCCT	1	1
CT	1	1
Bunch current monitor	1	1

The commissioning started with the tuning of the beam transfer lines. Injection to the LER started on Feb. 8th and beam was successfully stored on the 10th. The HER

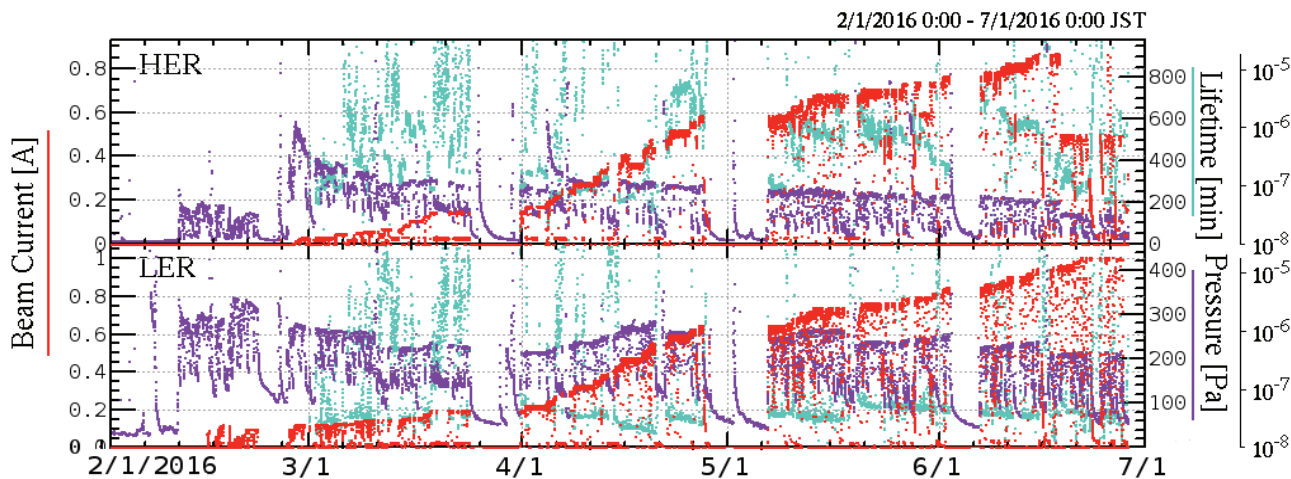


Figure 1: Beam history of Phase 1 operation of SuperKEKB rings. Red: Beam current, Purple: Average vacuum pressure (Pa), Cyan: Beam lifetime (min).

injection tuning started on Feb. 22nd and the beam was stored on the 25th. After the successful beam storage of both rings, we checked the BPM response, corrected the beam optics to reduce deviations from the design, then fairly conservatively increased the beam current, about 20 mA/day while carefully monitoring the status of vacuum components. Maximum beam currents of 1010 mA and 870 mA in LER and HER have been achieved. The integrated beam dose amounted to 768 Ah and 658 Ah for LER and HER, respectively, which fulfil the requirements from the Belle-II Group.

BEAM POSITION MONITORS

Though most of the vacuum chambers including BPM chambers of HER are the same as used in KEKB, we have replaced most of the LER vacuum chambers with an ante-chamber structure to suppress electron cloud build-up. As the cutoff frequency of the chamber became lower than the detection frequency (1 GHz) of the old narrowband detector used at KEKB [3], we have developed 509 MHz narrowband detectors, and separated the LER and HER detection systems. We have also developed gated turn-by-turn monitors [4,5] inserted between the buttons and the narrowband detectors, which are selectable by the optics group. Figure 2 shows the block diagram of the BPM systems.

Cable connections from BPM heads to the detectors at local control rooms have been checked using the beam. In total, 25 misconnections have been found and one damaged SMA connector has been found. The misconnections have been repaired at the maintenance time during Phase-1 operation. The damaged SMA connector was also replaced after operation.

Button Electrode and BPM Chamber

Most of the BPM chambers and button electrodes in the HER have been reused from KEKB, with the diameter of the button of 12 mm, and the N-type connector. For LER and new HER chambers, a button electrode with a diameter

of 6 mm and with reverse-SMA connector has been developed with a flange type structure [6]. The rotation angles of the BPM chambers were measured prior to operation and the RMS value was 0.62 mrad and 0.78 mrad for HER and LER, respectively. This data has been included in the position calculation of the narrowband systems.

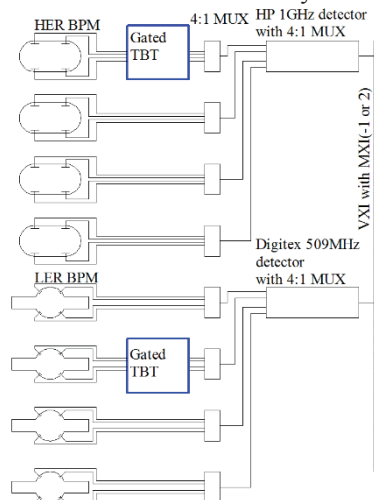


Figure 2: Block diagram of beam position monitors.

Narrowband Systems

The KEKB detectors were 1 GHz super-heterodyne detectors with the form factor of VXI-C. They are re-used in most of the HER BPMs and some of the LER BPMs at RF sections. For new chambers with a lower cut off frequency, new 509 MHz super-heterodyne detectors have been developed and installed.

In the early stage of the commissioning, we have observed an anomalous increase of the detected signal level of 1 GHz detectors around the RF section without beam, which might be caused by leakage fields from the RF high power stations. In the 509 MHz detector, no such signal has been observed, which shows the much better RF shielding characteristics of the new system.

The gain differences between the four electrodes have been calibrated using the beam with the gain mapping method [7]. Figure 3 shows an example of the result of gain mapping of LER relative to electrode A. Since most of the LER electrodes are installed on the monitor chamber with a flange connection, it shows a somewhat worse distribution than that of the HER, where electrodes were brazed to the monitor chambers. The change of the gains has been monitored by using the "consistency calculation method" where the rms of four beam positions solved by using combination of 3 electrodes were checked. The HER BPM showed worse behaviour where old N-type connectors have been used.

The BPM centers relative to the adjacent quadrupole magnetic centers have been measured by the beam based alignment method. The rms values of the offset (x, y) were 0.570 mm/0.222 mm in LER, and 0.505 mm/0.392 mm in HER. After the correction of the gain and the real center of the BPM, the optics group successfully corrected the beam optics with correction magnets prepared using the model assumptions.

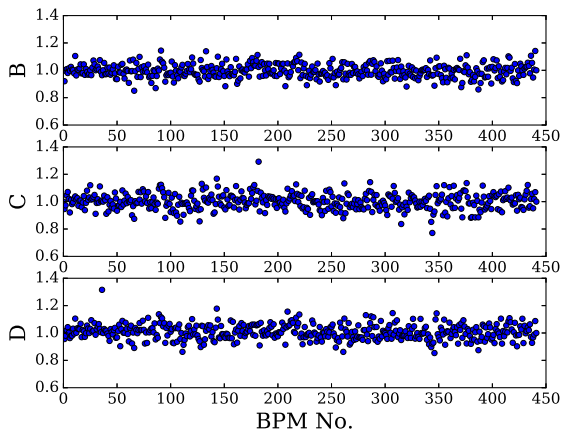


Figure 3: Example of BPM gain mapping of LER relative to electrode A.

The resolution of the narrowband BPM has been measured with the "3-bpm method," which measures correlations of the orbit among three BPMs. Obtained resolution is better than 3 μm and 5 μm in the LER and HER, respectively, for most of the BPMs. As the result will be affected by beam movement between the switching interval of the multiplexer, and as the amplitude of observed real beam motion around 9 Hz was of the order of a few μm , this rather larger value does not representing the real performance of the detector. We have also measured the current dependence of the resolution from 20 mA to 80 mA and found almost no dependence.

Gated Turn-by-Turn Monitor

We have developed the gated turn-by-turn monitor (GTBT) mainly to measure the beam optics (phase advance between the BPMs) during the collision using non-colliding bunch without feedback, and to measure the injection beam orbit [4, 5]. It has four independent channels, each of

them consisting of a fast RF switch, a log-ratio beam signal detector, and a 14-bit ADC. A photo of the GTBT is shown in Fig. 4.

Since it is almost impossible to adjust the timing of the GTBTs before the beam circulation of the rings, we at first struggled to adjust the ADC timing with the injection beam with the signal gate fully opened. Also very unfortunately, as the distribution of the GTBT was not dense enough around the injection point, we needed to connect fast oscilloscopes to several BPMs to see the injection beam before the next GTBT. After most of the ADC timings were roughly adjusted, they contributed to tuning injection, especially in the HER where the betatron tune fell into the stopband, preventing longer beam circulation. Figure 5 shows an example of intensity and position of the injected beam in the HER. After beam storage, we adjusted fine ADC and gate timing. The optics measurement with GTBTs using single-bunch beam excitation was also attempted. The analysis is in progress.



Figure 4: Photo of the gated turn-by-turn detector.

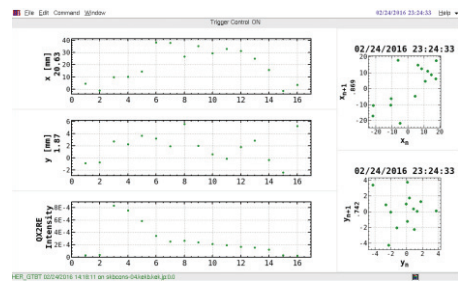


Figure 5: Example of turn-by-turn data at HER injection.

Low frequency beam oscillation was measured in several BPMs with long-duration recording (1.3 s) of the GTBTs. Figure 6 shows an example of an FFT of the vertical beam position of a BPM at a normal arc section. At lower frequency two peaks (9.1 Hz and 16.68 Hz) exist with an amplitude of around 5 μm .

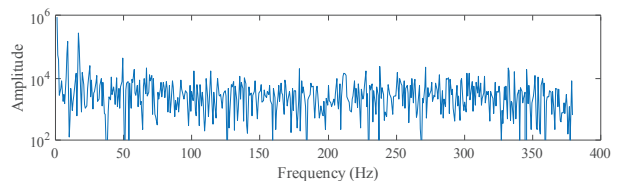


Figure 6: FFT of vertical beam position. Amplitude at 16.68 Hz was about 5 μm .

BUNCH FEEDBACK SYSTEMS

Figure 7 shows the block diagram of the bunch-by-bunch feedback systems installed in SuperKEKB rings [8]. The system consists of position detection systems, high-speed digital signal processing systems with a base clock of 509 MHz (iGp12 [9]), and wide-band kickers fed by wide-band, high-power amplifiers.

In the very early stage of the commissioning of both rings, we encountered very strong transverse coupled-bunch instabilities which limited the maximum beam currents. We have roughly adjusted the feedback timing including one-turn delay, feedback gain and feedback phase by seeing the beam response on an oscilloscope, then closed one loop per plane on each ring. The instability was successfully suppressed and the beam current was increased fairly smoothly, which contributed greatly to vacuum scrubbing.

During the scrubbing of the LER with a current of more than 660 mA, we encountered an unexpected longitudinal broadband coupled-bunch instability. We quickly tuned the longitudinal feedback system of LER. Though the fine tuning was not optimized, we successfully suppressed the instability up to the maximum beam current of the LER.

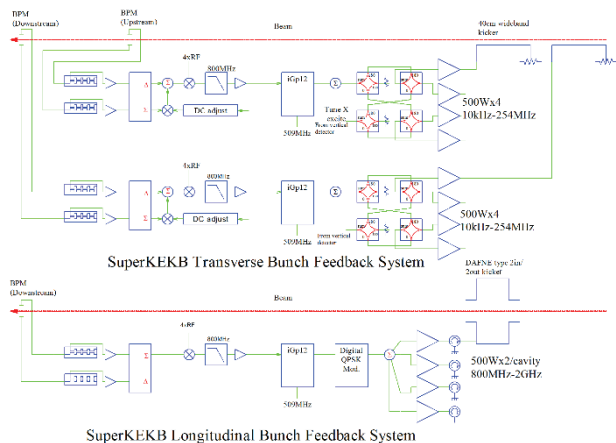


Figure 7: Block diagram of the transverse and longitudinal bunch feedback systems.

After fine-tuning all the feedback components, we made transient-domain measurements of the system [10]. Figure 8 shows an example of the evolution of unstable modes in a grow-damp experiment at the LER with a by-2 filling pattern where the total recording time, FB-off start and FB-off time are 24.72 ms, 2ms and 8ms, respectively. The unstable modes and exponential growth suggest this instability comes from electron-cloud instabilities.

In the HER, the growth time of the instability seemed to be governed by the vacuum condition, not only the mean vacuum pressure but also the worst vacuum pressure in the ring. The slowing-down behaviour of evolution of unstable modes suggests it is caused by ions, such as a fast ion instability. The nominal feedback damping time at the beam current of near 1 A was about 0.5 ms in both rings.

By using the bunch feedback technology, we have prepared the following instrumentation: the bunch current

monitor (BCM), the bunch oscillation recorder and the betatron tune monitor. In the BCM, we stopped the recoding with the injection trigger. The ADC data are also written to a reflective memory which automatically transfers the data to the connected board at the bucket selection system, which selects the next injection bucket within 20 ms. With this bunch current equalizer, very flat filling pattern have been realized during Phase 1 operation.

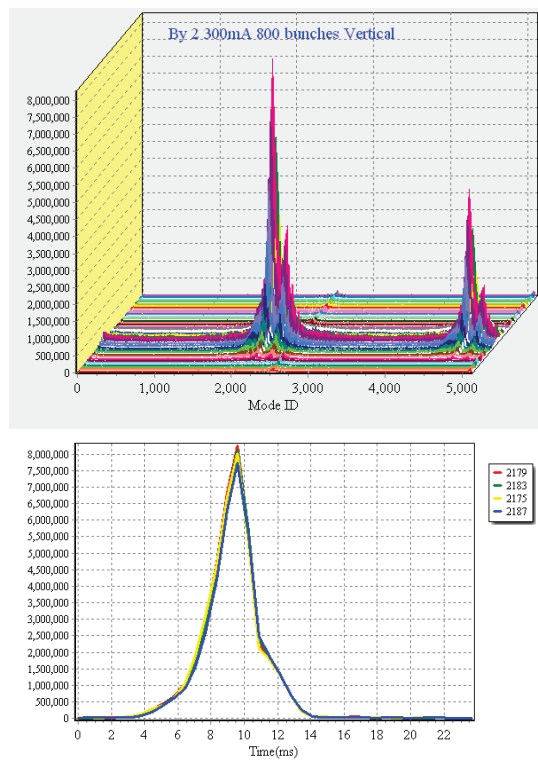


Figure 8: Evolution of vertical unstable modes with by-2 pattern in LER at a current of 300 mA. The growth time constant of mode 2179 was about 1.2 ms and the feedback damping time was about 1.1 ms.

For the betatron tune measurement, during the low beam current, we excite all bunches using the feedback kicker with the frequency down-converted from the tracking generator of a spectrum analyser while monitoring the beam signal from a feedback button electrode. This response becomes wider with the feedback damping so it is not applicable in high beam current conditions of, for example, larger than 50 mA.

In the single bunch measurement, we use an iGp12 to close the phase-locked loop excitation for a selected bunch without feedback damping. The betatron frequency is directly measured by the excitation frequency of the loop.

During operation, we found an increase in the reflected power from several rods of the transverse feedback kickers, which might be the result of rod damage in the kicker. Since the feedback damping was sufficient in the Phase 1 operation, we temporarily changed the power line from amplifier to high power attenuator, and continued the operation. After the end of Phase 1 running we inspected all the

components by TDR and found loosely connected N-connectors, and damaged high power attenuators. No suspicious symptoms have been found in the kicker and cables. Nevertheless, we are planning to open the kickers to inspect them directly.

PHOTON MONITORS

X-ray Monitor

X-ray monitors (XRM) are installed in both rings, primarily for vertical beam size measurements. Three sets of optical elements, made of gold masking on diamond substrates, are available at each ring: a single 33 μm slit, a multi-slit coded aperture, and a URA coded aperture [11]. From Phase 2 of SuperKEKB operations, a fast pixel detector for bunch-by-bunch, turn-by-turn measurements is planned. For Phase 1 of SuperKEKB operations, the detector consists of a YAG:Ce scintillator observed by a CCD camera, with which commissioning of the x-ray beam lines and calibration studies [12] were carried out, as well as bunch- and turn-averaged emittance measurements and electron-cloud blow-up studies. Figure 9 shows an example of electron-cloud blow-up data taken at the LER. For details on the calibration studies carried out, see [12], elsewhere in these proceedings. Detailed analysis of calibration data taken during Phase 1 is still underway.

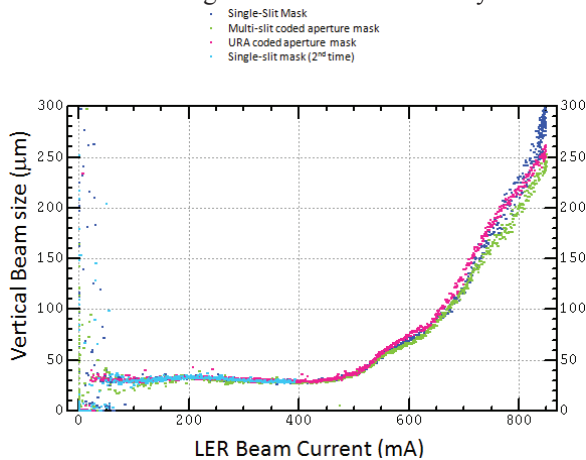


Figure 9. LER Vertical beam size as function of beam current, showing electron-cloud blow-up above 450 μm . Different colors represent data taken with different x-ray optical elements.

Synchrotron Radiation Monitor

The synchrotron radiation monitors (SRMs) use visible synchrotron radiation for use by interferometers, primarily for horizontal beam size measurement, and streak cameras, for bunch length measurement. The visible light lines were commissioned and aligned during Phase 1. Figure 10 shows an example of bunch lengths measured as functions of LER and HER bunch currents.

Large-Angle Beamstrahlung Monitor

A Large-Angle Beamstrahlung Monitor (LABM) has been installed to measure the polarization components of

the synchrotron-like radiation emitted by beam-beam collisions, from which mismatches in beam sizes, offsets and orientations can be detected for luminosity tuning. There were no beam collisions in Phase 1, but the LABM system was tested and successfully observed synchrotron radiation that passed through the interaction point from bending magnets upstream of the IP.

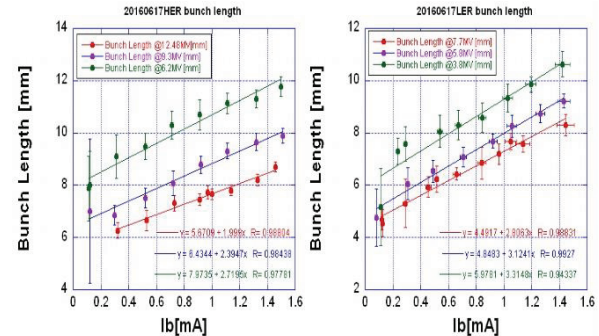


Figure 10: Bunch lengths as functions of bunch currents at HER (left) and LER (right) for different RF voltages. Measurements were made using streak cameras.

SUMMARY

Beam instrumentation systems for SuperKEKB rings have been constructed and commissioned. All the system has shown excellent performance and helped to realize fairly smooth beam commissioning of the rings.

The authors would like to express their sincere appreciation to Dr. A. Drago for his deep contributions of the commissioning. They thank the commissioning group of SuperKEKB for their help in the operation.

REFERENCES

- [1] Y. Funakoshi, *et al.*, in proceedings of IPAC 2016, TUOBA01, 2016, Busan, Korea.
- [2] Y. Funakoshi, private communication.
- [3] M. Arinaga, *et al.*, Prog. Theor. Exp. Phys. (2013) 03A007.
- [4] M. Tobiyama, *et al.*, in proceedings of IBIC 2013, MOPF32, 2013, Oxford, GB.
- [5] M. Tobiyama, in proceedings of IBIC 2014, WEPD05, 2014, Monterey, CA, U.S.A.
- [6] M. Tobiyama, *et al.*, in proceedings of BIW10, TUPSM041, Santa Fe, NM, U.S.A.
- [7] M. Tejima, in proceedings of IBIC 2015, TUBLA01, 2015, Melbourne, Australia.
- [8] M. Tobiyama, *et al.*, in proceedings of 13th Annual Meeting of Particle Accelerator Society of Japan, TUOM06, Makuhari, 2016, Japan.
- [9] DimTel, <http://www.dimtel.com>
- [10] J. D. Fox, *et al.*, in proceedings of the 1999 PAC, New York, NY, p.636.
- [11] E. Mulyani and J.W. Flanagan, in proceedings of IBIC 2015, Melbourne, p.377 (2015).
- [12] E. Mulyani and J.W. Flanagan, TUPG72, in proceedings of IBIC 2016, Barcelona, Spain.